



## Glutathione S-transferase Mu 2 inhibits hepatic steatosis via ASK1 suppression

Yi Jin<sup>1,2</sup>, Yanjie Tan<sup>1</sup>, Pengxiang Zhao<sup>1</sup>, Yu Guo<sup>1</sup>, Shilin Chen<sup>1</sup>, Jian Wu<sup>1</sup> & Zhuqing Ren<sup>1,2</sup>

Hepatic steatosis is the main characteristic of some liver metabolism diseases. However, unclear molecular mechanism of hepatic steatosis impedes the therapy of this hepatic steatosis. Glutathione-S-transferase mu 2 (*GSTM2*), as a member of phase II drug metabolizing enzymes (DMEs), regulates cellular antioxidant and detoxificant. *GSTM2* was highly up-regulated in hepatic steatosis tissues and high-fat diet (HFD) fed mice. Loss-of-function *GSTM2* mouse model demonstrated that *GSTM2* protected mice from excess fat accumulation. Mechanistically, *GSTM2* interacted with ASK1 and suppressed its phosphorylation and the activation of subsequent downstream p38-JNK signalling. Moreover, *GSTM2* over-expression in the liver effectively ameliorated hepatic lipid accumulation. Therefore, we identified *GSTM2* as an important negative regulator in progression of hepatic steatosis via both its detoxification/antioxidant and inhibition of ASK1-p38/JNK signalling. This study showed potential therapeutic function of the DME in progression of hepatic steatosis.

<sup>1</sup>Key Laboratory of Agriculture Animal Genetics, Breeding and Reproduction of the Ministry of Education & Key Laboratory of Swine Genetics and Breeding of the Ministry of Agriculture, College of Animal Science, Huazhong Agricultural University, Wuhan, Hubei 430070, PR China. <sup>2</sup>Hubei Hongshan Laboratory, Wuhan, Hubei 430070, PR China. ✉email: [wujian@mail.hzau.edu.cn](mailto:wujian@mail.hzau.edu.cn); [renzq@mail.hzau.edu.cn](mailto:renzq@mail.hzau.edu.cn)

**H**epatic steatosis, characterized by excessive accumulation of triglycerides (TGs) in hepatocytes, is considered the cause of non-alcoholic fatty liver disease (NAFLD)<sup>1–3</sup>. Disordered lipid metabolism leads to the hepatic steatosis causing lots of excess fat accumulation in hepatocytes. High hepatic fat content is the important inducement of the impairment of redox imbalance and insulin resistance. However, the molecular mechanisms of hepatic steatosis occurrence and progression are poorly understood.

Drug-metabolising enzymes (DMEs) play an important role in scavenging the waste products of lipid metabolism and oxidative metabolism and maintaining homeostasis of liver<sup>4,5</sup>, consisted of groups of enzymes, such as glutathione S-transferases (GSTs). Several studies reported DMEs could respond to the hepatic steatosis by protecting hepatocytes from free radicals<sup>6,7</sup>, additionally, GSTs are always considered as the scavenger of reactive oxygen species. Among other GSTs, glutathione S-transferase M2 (*GSTM2*) seems to be different. Previous researches from Huenchuguala et al. reported that they found cells with *GSTM2* knockdown accumulated more lipid droplets<sup>8–11</sup>. Moreover, *GSTM2* was highly up-regulated in high-fat diet mouse liver<sup>6,7</sup>. These studies suggested *GSTM2* regulated lipid metabolism specially beyond detoxification/antioxidant, the basic functions of GSTs.

In the present study, the close association between *GSTM2* knockout and hepatic steatosis was examined by using *GSTM2*-null mice. We demonstrated that *GSTM2* protects against hepatic steatosis by inhibiting excess fat accumulation by interacting with and suppressing activation of apoptosis signal-regulating kinase1 (*ASK1*) and subsequent p38-JNK signalling, besides its antioxidant capacity. Moreover, *GSTM2* overexpression reversed methionine choline-deficient diet (MCDD)-induced steatosis. Thus, we identified *GSTM2* as an important negative regulator in hepatic steatosis progress.

## Results

***GSTM2* was upregulated in hepatic tissues of mice fed HFD and MCDD.** The high-fat diet and methionine choline deficient diet were used to make hepatic steatosis. We validated the expression pattern of *GSTM2* in the HFD and MCDD mouse models. The level of *GSTM2* mRNA and protein were detected. *GSTM2* was significantly up-regulated in mice fed HFD (Fig. 1a–c) and MCDD (Fig. 1d–f).

### ***GSTM2* deletion strongly promotes hepatic fat accumulation.**

To investigate the function of *GSTM2* in the progression of hepatic steatosis, we generated a *GSTM2* knockout (*GSTM2* KO) mouse (Supplementary Fig. 1a, b). Hepatic histomorphology and TG content detection showed that *GSTM2* KO mice had higher hepatic fat content (Fig. 1g, h). Moreover, there was no significant difference in the ratio of liver weight to body weight between *GSTM2* KO and WT mice (Supplementary Fig. 1c, d). We also investigated the fat content in white adipose and skeletal muscle tissues via Oil Red O staining. More intramuscular fat was observed in *GSTM2* KO mice, whereas no significant difference was found in white adipose tissue between KO and WT mice (Supplementary Fig. 1e, f). To further investigate the function of *GSTM2* in hepatic lipid metabolism, we challenged the mice with HFD. KO mice accumulated more fat at a faster rate than WT mice (Fig. 1i, j, Supplementary Fig. 1g). Moreover, the hepatic alanine aminotransferase (ALT) level was higher in KO mice, while the  $\gamma$ -glutamyltranspeptidase (GGT) level was not changed (Supplementary Fig. 1h, i). We next challenged the mice with 0.2 mM oleic acid medium (dissolved by BSA in 0.9% NaCl solution) to investigate the effect of *GSTM2* on the rapid

formation of LDs. Hepatic morphology analysis showed that *GSTM2*-KO-livers formed more LDs than WT livers (Supplementary Fig. 1j, k). These results suggest that *GSTM2* plays an important role in excess hepatic fat accumulation.

***GSTM2* overexpression suppresses hepatic steatosis.** Although *GSTM2* was up-regulated in mice with hepatic steatosis, we also overexpressed this protein in mouse model fed with MCDD (Supplementary Fig. 2a). Western blot analysis showed that *GSTM2* was highly expressed in liver tissues (Supplementary Fig. 2b). As the feeding time increased, control mice accumulated much more hepatic fat, while *GSTM2* overexpression suppressed hepatic fat accumulation (Fig. 2a). Control mice showed significant hepatic steatosis after 1 week of MCDD feeding, whereas mice with *GSTM2* overexpression showed this effect at 4 weeks. Additionally, *GSTM2*-overexpressing mice showed mild LD accumulation in the first 3 weeks (Fig. 2b). Because fibrosis is the key signal of steatosis aggravation, we further detected the fibrosis level in liver tissues. Masson staining analysis indicated that control mice had significant hepatic fibrosis compared to mice with *GSTM2* overexpression (Supplementary Fig. 2c, d). A significant degree of fibrosis was observed in liver tissues of control mice at 3 weeks, whereas *GSTM2*-overexpressing mice showed mild fibrosis at 8 weeks (Supplementary Fig. 2c, d). Moreover, we detected the marker genes of fibrosis  $\alpha$ -SMA and *Col1A1*. The results showed the expression of  $\alpha$ -SMA and *Col1A1* was up-regulated at 8 weeks significantly (Supplementary Fig. 2e). These results suggest that *GSTM2* overexpression inhibits hepatic steatosis development. We subsequently performed a rescue test. A *GSTM2* overexpression vector was transfected into mice fed MCDD for 2 weeks, which was then changed to a chow diet (Supplementary Fig. 2f). Overexpression efficiency was detected by Western blotting (Supplementary Fig. 2g). As expected, *GSTM2* overexpression promoted the recovery of hepatic steatosis compared to control (Fig. 2c). Although both *GSTM2*-overexpressing mice and control mice showed good recovery of hepatic steatosis at 2 weeks, *GSTM2*-overexpressing mice showed lower hepatic fat content at 1 week (Fig. 2d). The rescue experiment suggests that *GSTM2* may be a useful therapeutic target for hepatic steatosis.

***GSTM2* modulates size and number of LDs in HepG2 cells.** To further investigate the potential regulatory mechanism, we generated a *GSTM2*-knockdown stable cell line (sh*GSTM2*-HepG2) that expressed less *GSTM2* mRNA and protein than control cells (shNC-HepG2) (Fig. 3a, b). Interestingly, sh*GSTM2*-HepG2 cells contained more LDs (~5 to 6 fold) in normal culture than shNC-HepG2 cells (Fig. 3c, d) and formed more and larger LDs (>2  $\mu$ m) under fatty acid (FA)-rich (200  $\mu$ M oleic acid medium) culture conditions (Fig. 3e, f).

### **Effects of *GSTM2* on LD content do not absolutely depend on regulating ROS level.**

Because *GSTM2* has antioxidant activity (as described in the Introduction), the potential effect of ROS on cellular lipid formation should be examined. We determined ROS levels in sh*GSTM2*-HepG2 and shNC-HepG2 cells in normal and FA-rich culture medium, respectively. As expected, the ROS level was significantly increased (~15–20%) by *GSTM2* knockdown ( $p < 0.01$ ) (Fig. 3g). We further investigated whether the increased cellular ROS levels affected the LD content by treating cells with an ROS activator (ROSup). As predicted, more cellular LDs (~2 to 3 fold compared to control) were observed in ROSup-treated cells (Fig. 3h, i). Indeed, the higher ROS level increased the LD number, but only approximately 30 LDs were observed in ROSup-treated cells (Fig. 3i), which was much lower than the

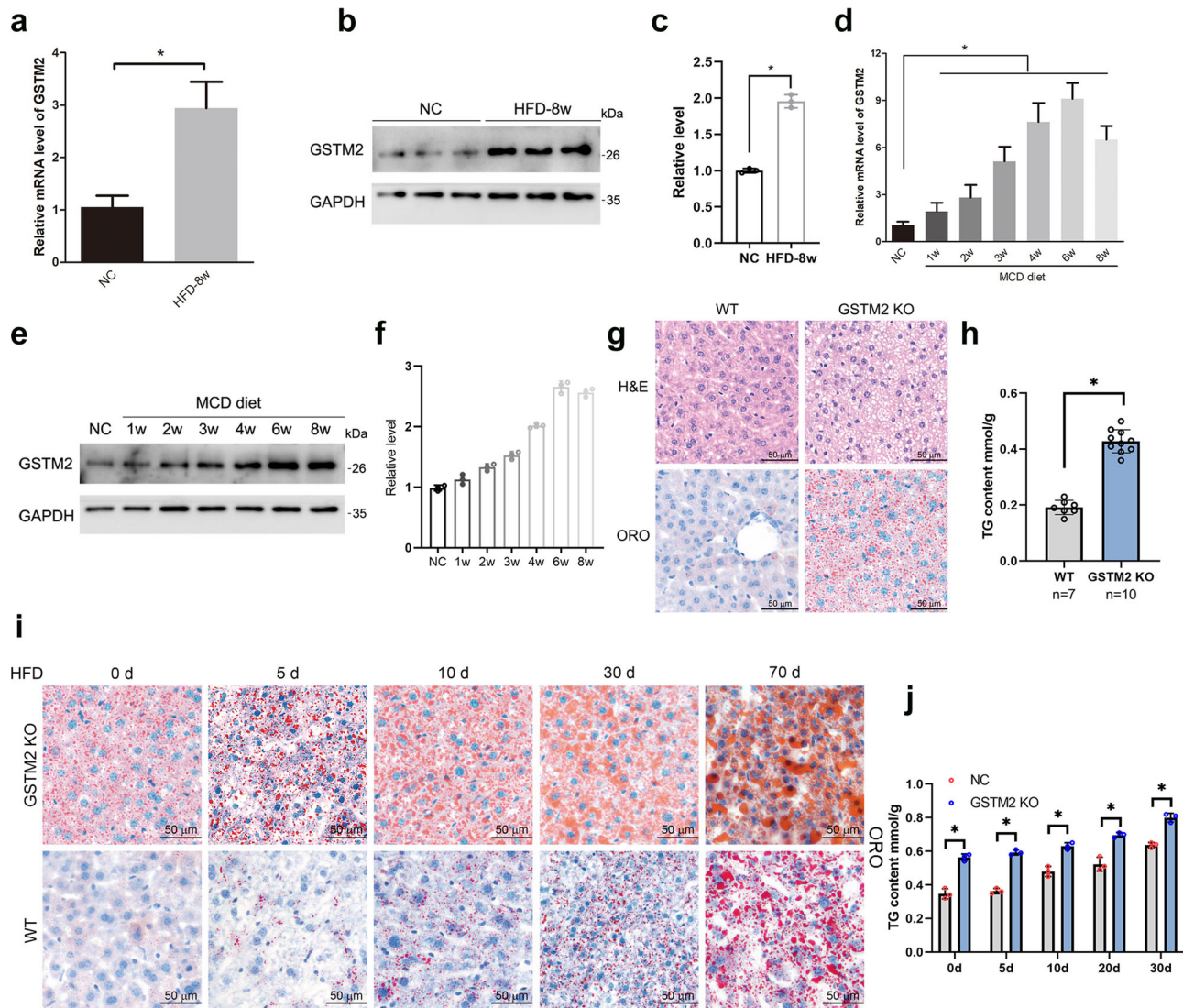


**Fig. 1** Loss-of-function of *GSTM2* promoted hepatic fat storage. **a–c** *GSTM2* mRNA and protein expression in liver samples of 8-week HFD fed mice ( $n = 3$ ) and 8-week chow diet fed mice ( $n = 3$ );  $*p < 0.05$ . **d–f** *GSTM2* mRNA and protein expression in liver samples of MCD fed mice and corresponding control mice;  $*p < 0.05$ . GAPDH served as the reference gene. **g** Haematoxylin and eosin (HE) and Oil red O staining analysis of liver samples of *GSTM2* knockout (KO) and control mice; bar = 20  $\mu\text{m}$ . **h** Hepatic TG concentrations of WT ( $n = 7$ ) and *GSTM2* KO ( $n = 10$ ) mice were detected;  $***p < 0.001$ . **i** Oil red O analysis of liver samples of *GSTM2* KO and control mice challenged with HFD at 0 d, 5 d, 10 d, 20 d, and 30 d. **j** Hepatic TG concentrations of WT and *GSTM2* KO mice with high-fat diet treatment at 0 d, 5 d, 10 d, 20 d, and 30 d;  $*p < 0.05$ . bar, 50  $\mu\text{m}$ .

number detected in sh*GSTM2*-HepG2 cells. Therefore, the increase in ROS did not greatly alter the cellular LD content.

We next investigated the changes in LD formation and expression of breakdown-related genes at different ROS levels. The expression of *PLIN2*, *PLIN5*, and *ATGL* was significantly increased by ROSup treatment ( $p < 0.05$ ) (Supplementary Fig. 3a). *PLIN2*, *PLIN3*, and *SREBF1* increased and *PCYT1A* decreased significantly following *GSTM2* knockdown ( $p < 0.05$ ) (Supplementary Fig. 3b). As expected, *GSTM2* overexpression significantly reduced the cellular ROS level (Supplementary Fig. 3c); therefore, we examined gene expression changes after *GSTM2* overexpression. In contrast to the results of *GSTM2* knockdown, *PLIN2* and *SREBF1* were down-regulated and *PCYT1A* was up-regulated, showing significant differences ( $p < 0.05$ ) (Supplementary Fig. 3d). Because *N*-acetylcysteine (NAC) is an effective ROS scavenger (Supplementary Fig. 3e), we investigated whether a reduced ROS level would alter the LD content by treating cells with 1 mM NAC. Interestingly, NAC did not significantly change

the number of LDs in either normal or FA-rich cultural medium (Supplementary Fig. 3f, g). To evaluate the contribution of the *GSTM2* oxidative ability in promoting LD formation, we added ROS scavenger (NAC) in *GSTM2* knockdown cells and detected the LD number. The result showed that NAC did suppress the LD number induced by *GSTM2* knockdown (Supplementary Fig. 3h). However, the LD number in NAC treatment group was still more than NC group (Supplementary Fig. 3h). These results suggest that modulating ROS levels by *GSTM2* is not the only approach for regulating the cellular lipid content.

***GSTM2* modulates p38-JNK signalling by inhibiting ASK1 activity.** ASK1-p38/JNK signalling plays an important role in NAFLD development, thus we investigated whether this signalling was affected by *GSTM2* expression. The phosphorylation level of ASK1 was regulated by *GSTM2*. The p-ASK1 level was increased by *GSTM2* knockdown and decreased by *GSTM2*

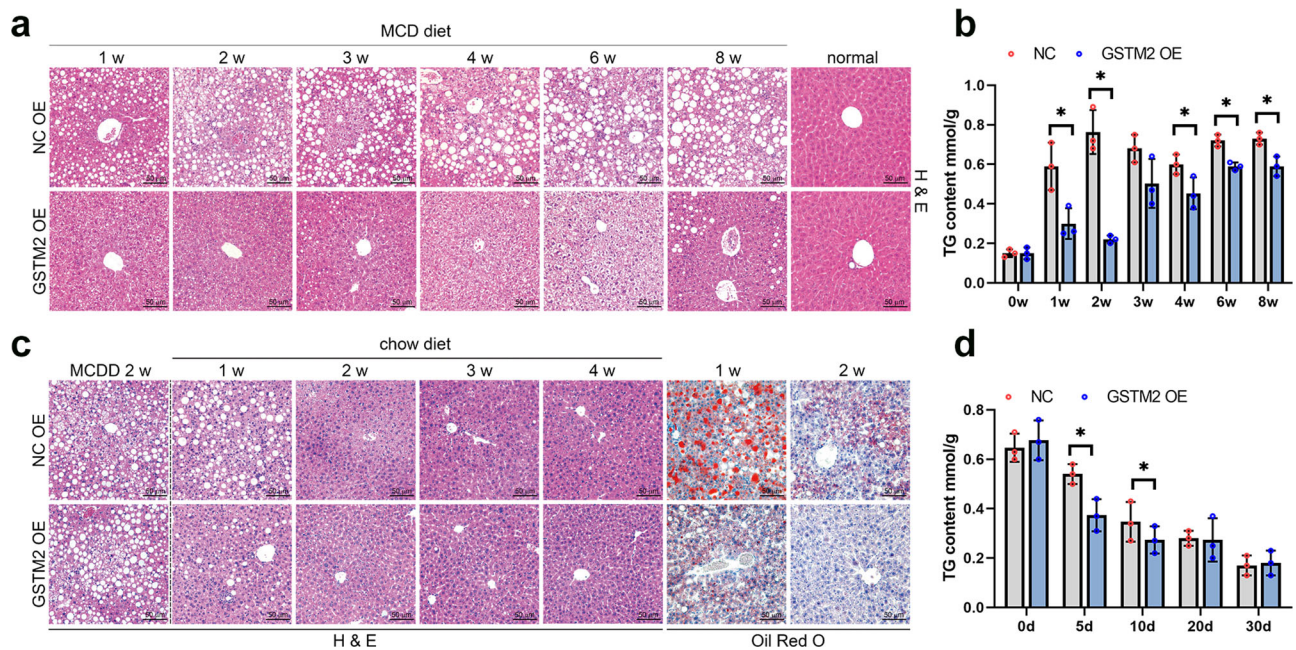


**Fig. 2** **GSTM2 overexpression protected against hepatic fat storage.** **a** HE staining analysis of liver samples of *GSTM2* overexpression (OE) and control mice challenged with MCD at 1 w, 2 w, 3 w, 4 w, 6 w, and 8 w. **b** Hepatic TG concentrations of *GSTM2* OE and control mice with MCD diet treatment at 0 w, 1 w, 2 w, 3 w, 4 w, 6 w, and 8 w; \**p* < 0.05. **c** Oil red O staining analysis of liver samples of *GSTM2* OE and control mice fed MCDD for 2 w and then chow diet. **d** Hepatic TG concentrations of corresponding mice in (c); \**p* < 0.05. bar, 50  $\mu$ m.

overexpression (Fig. 4a, b). Moreover, *GSTM2* knockdown and overexpression had different effects on p38-JNK signalling. The phosphorylation levels of p38 and JNK were increased by *GSTM2* knockdown, but decreased by *GSTM2* overexpression (Fig. 4d). We further examined the effect of *GSTM2* on ASK1-p38/JNK signalling in the presence of palmitic acid (PA), an ASK1 activator. As expected, *GSTM2* overexpression reduced ASK1 signalling activation (Fig. 4e). ASK1 signalling was activated and enhanced in liver tissues with the development of NAFLD<sup>12</sup>, which leads to severe inflammation and fibrosis. This result suggests that *GSTM2* has a potential therapeutic function in NAFLD.

**C-terminus of *GSTM2* inhibits ASK1 phosphorylation by binding to ASK1.** We then investigated the mechanism of *GSTM2* regulation of ASK1 activity. Previous studies reported that the C-terminus of *GSTM1* binds to ASK1 and suppresses the phosphorylation of ASK1<sup>13,14</sup>. Thus, we compared the amino acid sequences and 3D structures of these two proteins. *GSTM1* and *GSTM2* shared highly similar sequences and structures (Supplementary Fig. 4a, b), with >90% similarity. Moreover, another study reported that *GSTM2* binds to ASK1<sup>15</sup>. We next examined whether *GSTM2* interacts with ASK1 by conducting a co-immunoprecipitation assay. The result indicated that *GSTM2* binds to ASK1 (Fig. 4f). We then investigated the structural details of this binding interaction. *GSTM2* contains two main functional domains, GST-binding (N-terminal) and C-terminal domains (Supplementary Fig. 4c). Overexpression of the C-terminus of *GSTM2* decreased the p-ASK1 level, whereas N-terminal overexpression did not (Fig. 4g).

***GSTM2* regulates expression levels of SREBF1 and PLIN2.** SREBF1 and PLIN2 play important roles in cellular lipid metabolism. A previous study reported that SREBF1 is regulated by p38-JNK signalling<sup>16,17</sup> and PLIN2 expression is regulated by SREBF1. We detected the effects of *GSTM2* on the expression of

these two genes. As expected, the expression levels of SREBF1 and PLIN2 were increased by *GSTM2* knockdown and decreased by *GSTM2* overexpression (Fig. 4h, i). We confirmed the effects of these two genes on cellular LD content by overexpressing *SREBF1* and *PLIN2*. More LDs were observed in cells with both *SREBF1* and *PLIN2* overexpression (Fig. 4j, k). Next, GS-4997, a specific ASK1 inhibitor, was used to confirm that the expression of SREBF1 and PLIN2 is regulated by ASK1-p38/JNK signalling. SREBF1 and PLIN2 expression was decreased in cells treated with GS-4997 (Fig. 4l).

To further validate the role of ASK1 in *GSTM2* knockdown cells, we detected LDs number in *GSTM2* knockdown cells treated with GS-4997. The result showed that GS-4997 greatly decreased LDs number compared to *GSTM2* knockdown cells (Fig. 4m). We further detected the protein level of SREBF1 and PLIN2 in *GSTM2* knockdown cells treated with PA or GS-4997. The results indicated that PA increased the expression level of SREBF1 and PLIN2 (Fig. 4n), whereas GS-4997 suppressed the expression level of SREBF1 and PLIN2 (Fig. 4o). The results indicated that *GSTM2* regulated SREBF1 and PLIN2 expression by affecting ASK1 activity.

***GSTM2* modulates growth of LDs via ASK1-p38/JNK signalling.** The growth of LDs is important in increasing the cellular capacity for lipid storage. Previous studies demonstrated that *PCYT1A*, *GPAT4* and *DGAT2* are responsible for increasing the size of LDs<sup>18–20</sup>. The expression level of *PCYT1A* was positively correlated with *GSTM2* expression, which was confirmed by *GSTM2* knockdown and overexpression assays (Fig. 5a–c). Furthermore, *PCYT1A* knockdown induced the formation of larger LDs in FA-rich cultural medium (Fig. 5d). In addition to regulating LD growth, *PCYT1A* is related to LD fusion or coalescence. We examined the events involved in LD contact using a living cell station. The supplementary movie shows that *GSTM2* knockdown induced more LD–LD contact events (Supplementary movie S1) than in the control (Supplementary movie S2).

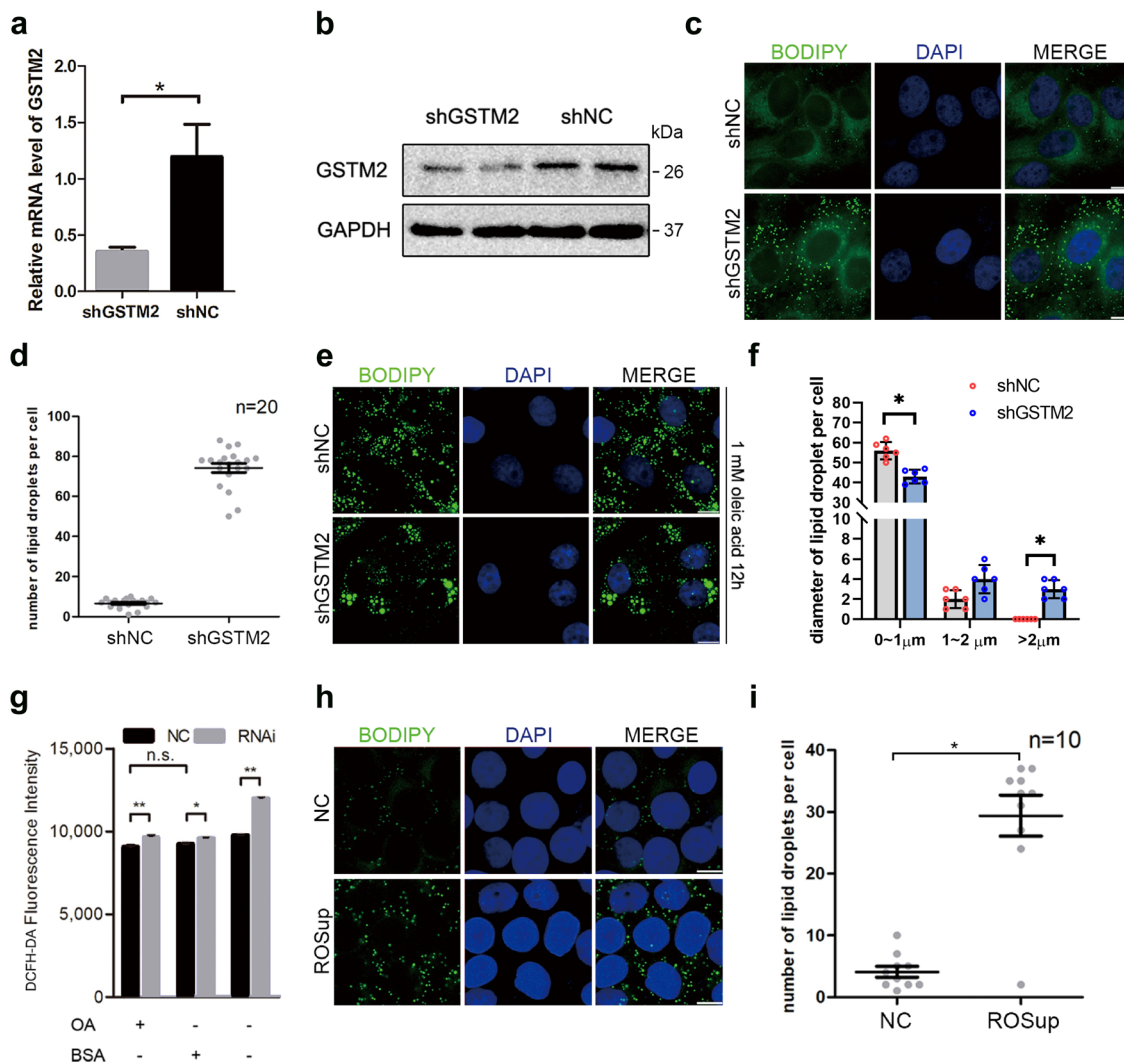


**Fig. 3** *GSTM2* modulated cellular lipid droplets accumulation via regulating cellular ROS level. **a, b** Expression level of *GSTM2* was detected in sh*GSTM2*-HepG2 cells and corresponding control cells. **c** More LDs were observed in sh*GSTM2*-HepG2 cells. **d** Statistics of LD number in sh*GSTM2*-HepG2 cells and shNC-HepG2 cells. **e** More larger LDs were found in sh*GSTM2*-HepG2 cells treated with 1 mM oleic acid medium for 12 h compared to control cells. **f** Statistics of LD diameter in sh*GSTM2*-HepG2 cells and shNC-HepG2 cells treated with 1 mM oleic acid medium for 12 h compared to control cells. **g** Cellular ROS level was detected in sh*GSTM2*-HepG2 and shNC-HepG2 cells in the presence or absence of oleic acid medium; \* $p < 0.05$ , \*\* $p < 0.01$ . **h** More LDs were observed in cells treated with ROSup compared to control cells. **i** Statistics of LD number in cells treated with ROSup and control cells. Bar, 10  $\mu\text{m}$ .

DGAT2 and GPAT4 targeting the surface of LDs is important for LD expansion. As described above, *GSTM2* modulated the size of LDs. We investigated whether this regulation was dependent on modulation of DGAT2 and GPAT4 targeting the LD surface. We found that more DGAT2 and GPAT4 were recruited to the LD surface by *GSTM2* knockdown (Fig. 5e, f). Next, we investigated the effect of ASK1-p38/JNK signalling on this progression. The expression level of DGAT2 and GPAT4 was detected in the presence of PA (ASK1 activator) or GS-4997 (ASK1 inhibitor) in normal or FA-rich cultural medium. The expression level of these protein was up-regulated by ASK1 signalling activation and down-regulated by ASK1 signalling suppression (Fig. 5g). Furthermore, recruitment of GPAT4 to the LD surface was enhanced by PA treatment and reduced by GS-4997 treatment (Fig. 5h). We further detected the effect of ASK1 activity on PCYT1A expression. The expression of PCYT1A was decreased by PA treatment, whereas was up-regulated by GS-4997 treatment (Fig. 5i, j,  $p < 0.05$ ).

***GSTM2* KO induced hepatic fat accumulation was suppressed by GS-4997 in vivo.** We then investigated whether GS-4997 treatment could rescue the hepatic steatosis induced by *GSTM2* knockout. *GSTM2* KO mice were treated with 80  $\mu\text{M}$  GS-4997 by intraperitoneal injection, and control mice were treated with an equal amount of DMSO solution (Fig. 6a). Then live tissues were collected and examined. We found that the GS-4997 treatment group showed less hepatic fat accumulation compared to the control group (Fig. 6b), and the TG content detection also supported this result (Fig. 6c). The results indicated that GS-4997 greatly suppressed the increase of TG accumulation induced by *GSTM2* KO. Moreover, we detected the p-ASK1 level in *GSTM2* KO mice, which showed the ASK1 was activated by *GSTM2* deletion (Fig. 6d). Previous study suggested that autophagy affected the TG utilization in liver<sup>21,22</sup>. We detected the expression level of LC3 in liver of *GSTM2* KO mice. The result showed the expression level of LC3-I and LC3-II was not changed in

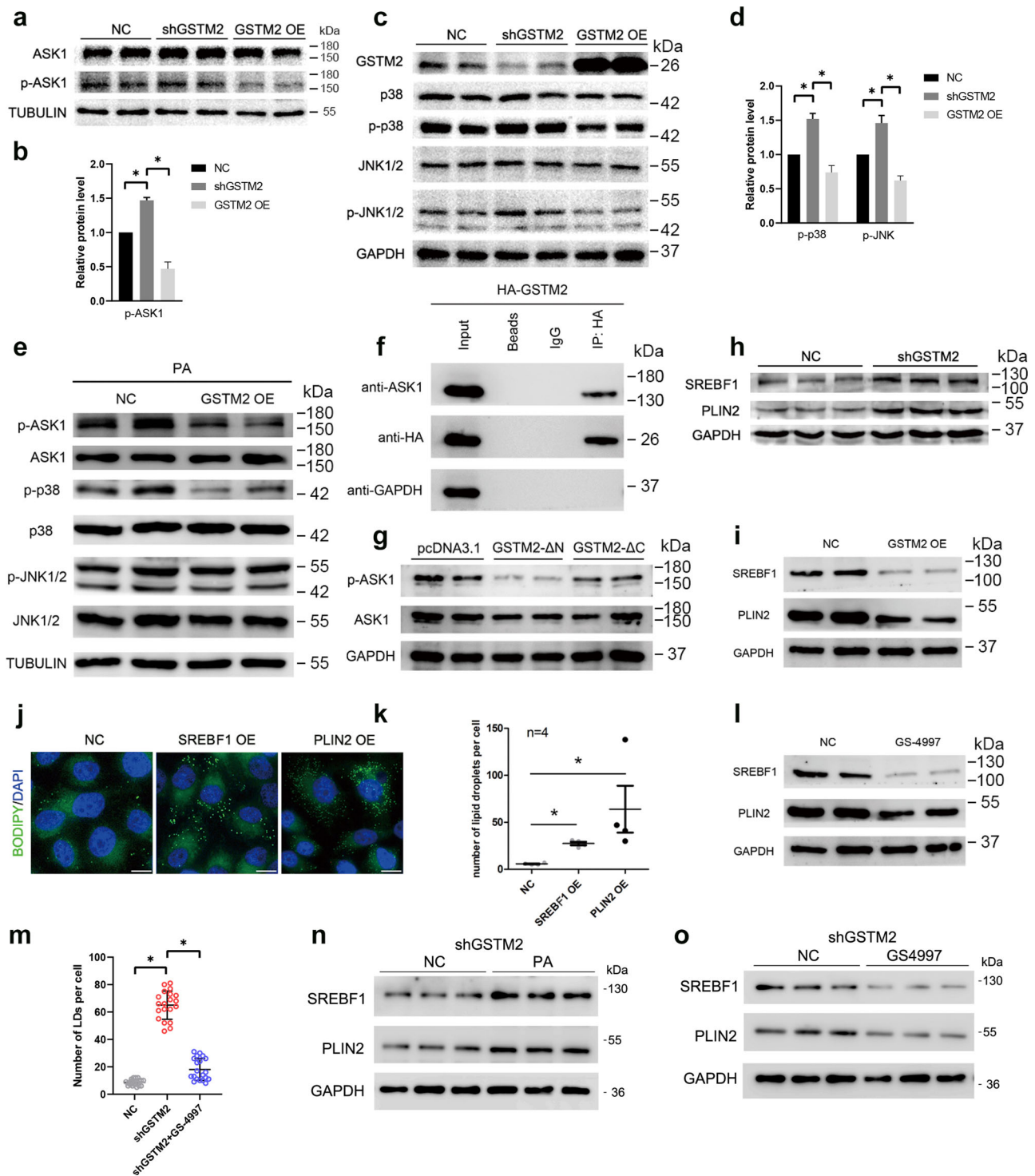


**Fig. 4** GSTM2 regulated lipid droplet accumulation via ASK1-p38/JNK signalling. **a, b** Phosphorylation of ASK1 was up-regulated by GSTM2 KD and down-regulated by GSTM2 OE. **c, d** p-p38 and p-JNK levels were up-regulated by GSTM2 knockdown (KD) and down-regulated by GSTM2 OE. **e** GSTM2 OE down-regulated ASK1-p38/JNK signalling in the presence of palmitic acid treatment. **f** GSTM2 interacted with ASK1 by co-IP detection. **g** GSTM2 C-terminal, not N-terminal, down-regulated ASK1 activity. **h** SREBF1 and PLIN2 expression level was up-regulated by GSTM2 KD. **i** SREBF1 and PLIN2 expression level was down-regulated by GSTM2 OE. **j** More LDs were observed in cells with SREBF1 or PLIN2 overexpression. **k** Statistical analysis of number of LDs in cells with SREBF1 or PLIN2 overexpression. **l** Expression levels of SREBF1 and PLIN2 were down-regulated by GS-4997 treatment (ASK1 activity inhibitor). **m** Statistical analysis of number of LDs in shGSTM2 cells and shGSTM2 cells treated with GS-4997. **n** WB detection of SREBF1 and PLIN2 in shGSTM2 cells treated with PA. **o** WB detection of SREBF1 and PLIN2 in shGSTM2 cells treated with GS-4997. Bar, 10  $\mu$ m.

GSTM2 KO mice (Fig. 6d). We then investigated the protein level of ASK1-p38/JNK signalling pathway. As expected, the levels of p-ASK1, p-p38 and p-JNK in the GS-4997 treatment group were decreased significantly ( $p < 0.05$ ) (Fig. 6e, f).

Subsequently, we detected whether GS-4997 treatment could block the progress of hepatic steatosis in KO and WT mice with MCD diet. The mice were fed with MCD for one month. During that time, GS-4997 was injected at 14 d, 21 d and 28 d (Fig. 6g). Then live tissues

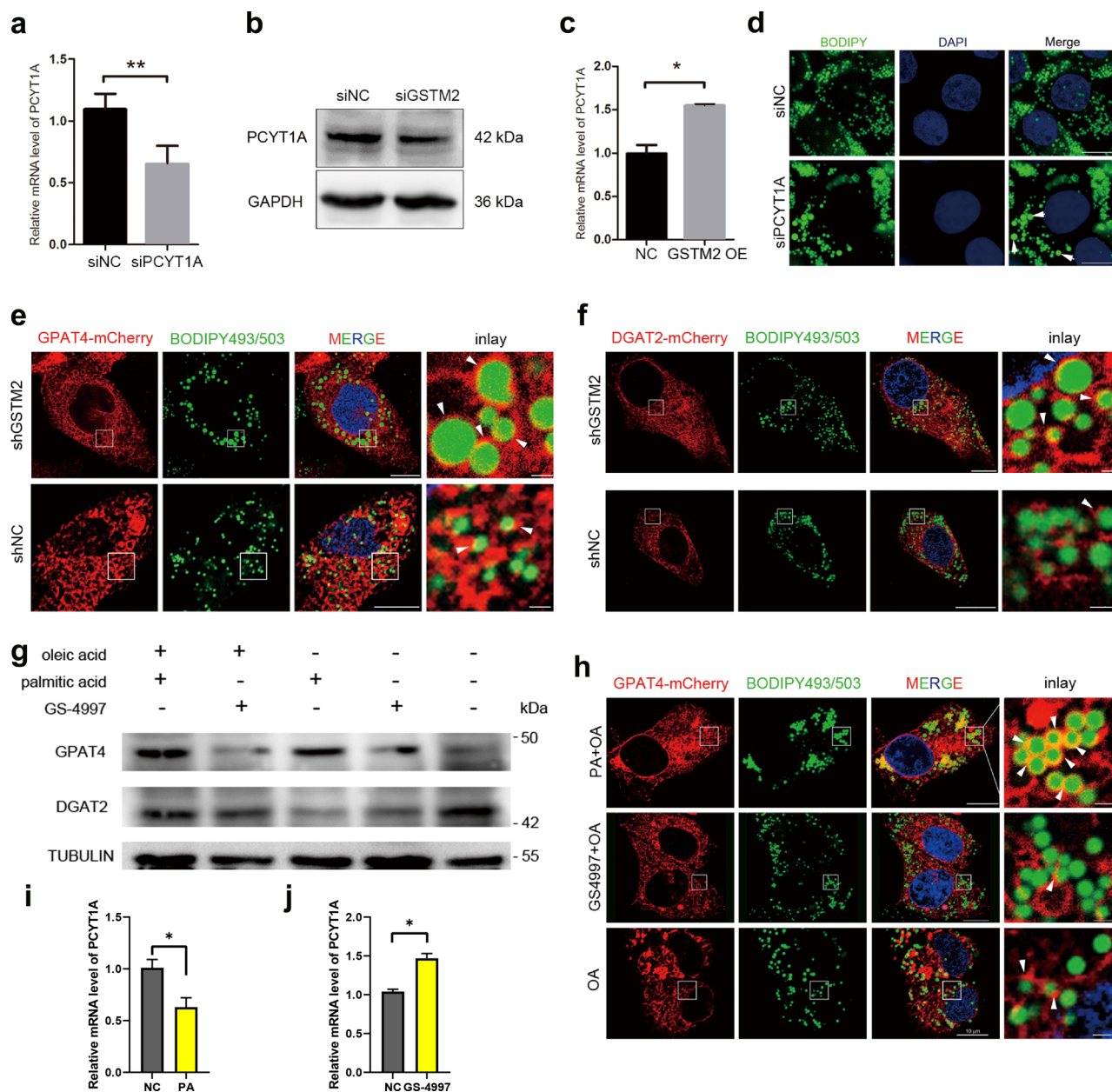


**Fig. 5** *GSTM2* modulated lipid droplet growth via ASK1 signalling. **a–c** PCYT1A expression level was down-regulated by *GSTM2* KD and up-regulated by *GSTM2* OE; \* $p < 0.05$ , \*\* $p < 0.01$ . **d** PCYT1A KD induced LD expansion. **e, f** *GSTM2* affected recruitment of GPAT4 and DGAT2 on LD surface (in the presence of oleic acid medium), bar, 10  $\mu\text{m}$ , 1  $\mu\text{m}$  (inlay). **g** Expression level of GPAT4 and DGAT2 was regulated by treatment of palmitic acid (ASK1 activator) and GS-4997 (ASK1 activity inhibitor). **h** Recruitment of GPAT4 on LD surface was regulated by palmitic acid or GS-4997 treatment, bar, 10  $\mu\text{m}$ , 1  $\mu\text{m}$  (inlay). **i, j** qPCR detection of PCYT1A expression with PA or GS-4997 treatment respectively.

were collected for further investigation. Histological examination showed that GS-4997 treatment decreased lipid accumulation in WT mice with MCDD (Supplementary Fig. 5a); additionally, the TG content in live tissues was also decreased compared to the DMSO treatment group (Supplementary Fig. 5b). The results of Western blot showed that p-ASK1, p-p38 and p-JNK protein levels were decreased significantly by GS-4997 injection in WT mice with MCDD ( $p < 0.05$ ) (Supplementary Fig. 5c). Furthermore, GS-4997 also inhibited fat accumulation in liver tissues of KO mice with MCDD (Fig. 6h). The TG content of the GS-4997 treatment group was decreased ( $p < 0.05$ ) (Fig. 6i). Moreover, the protein level of p-ASK1, p-p38 and p-JNK was decreased in KO mice with MCDD by GS-4997 treatment ( $p < 0.05$ ) (Supplementary Fig. 5d). Besides detecting the effect of GS-4997 treatment on hepatic fat accumulation, we also

investigated the degree of hepatic fibrosis of the samples. As expected, GS-4997 suppressed hepatic fibrosis in both WT and KO mice with MCDD (Fig. 6g, Supplementary Fig. 5a), as detected by Masson staining. These results support that *GSTM2* knockout induced hepatic steatosis resulting from ASK1 signalling activation and can be rescued by treatment with GS-4997, an ASK1 inhibitor, in vivo.

## Discussion

The risk of hepatic steatosis is greatly increased by an unhealthy lifestyle and excess energy intake. The regulatory mechanism of steatosis is unclear. Here, we showed that *GSTM2* negatively regulated hepatic steatosis. *GSTM2* inhibited p38 and JNK signalling by suppressing activation of the upstream kinase ASK1.

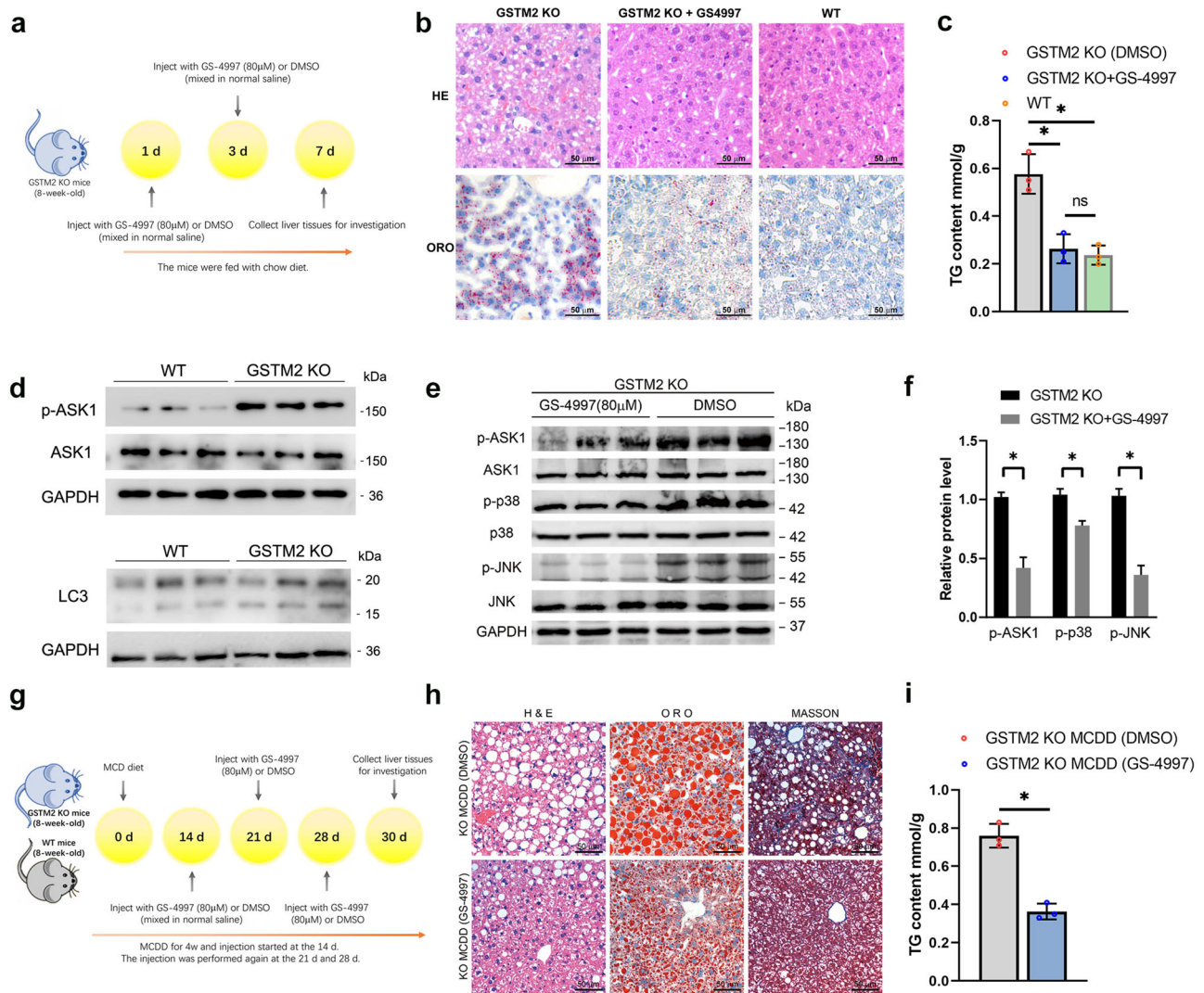


**Fig. 6** *GSTM2* KO induced hepatic fat accumulation was suppressed by GS-4997 in vivo. **a** The *GSTM2* KO mice were fed with chow diet and treated with GS-4997 or DMSO at day 1 and 3, then the liver tissues were collected for further analysis. **b** *GSTM2* KO mice were treated with GS-4997 (ASK-1 inhibitor) by intraperitoneal injection. Hepatic fat was detected by HE and ORO staining. **c** TG content examination of WT mice fed MCD with GS-4997 or DMSO treatment. **d** WB detection of expression level of p-ASK1 and LC3 in *GSTM2* KO mice liver. **e** Investigation of protein levels of ASK1 signalling pathway in *GSTM2* KO mice with GS-4997 or control, DMSO treatment by Western blot. **f** Fray value analysis of (**e**) by ImageJ software. **g** The WT and *GSTM2* KO mice were fed with MCD diet for one month. The mice were treated with GS-4997 or DMSO at day 14, 21 and 28, and then the liver tissues were collected for further Analysis. **h** *GSTM2* KO mice were fed MCD and treated with GS-4997 or DMSO by intraperitoneal injection. Then hepatic fat and fibrosis level were detected by HE, ORO and Masson staining. **i** TG content examination of *GSTM2* KO mice fed MCD with GS-4997 or DMSO treatment. bar, 50  $\mu$ m.

More importantly, we showed that overexpression *GSTM2* had a therapeutic effect on hepatic steatosis. Mechanistically, *GSTM2* modulated the formation of hepatic fat mainly by regulating the number and size of cellular LDs.

Few studies have evaluated the relationship of DME and hepatic steatosis. Our study demonstrated that the hepatic phase II DME, *GSTM2*, was involved in the development of hepatic steatosis. A previous study showed that hepatic steatosis increased the toxicity of hepatic drugs by down-regulating the expression of some DMEs<sup>23</sup>. Moreover, many studies showed that hepatic steatosis increased the risk of drug-induced liver disease<sup>24–27</sup>. hepatic steatosis may impair hepatic self-protection. Previous studies reported that *GSTM2* is highly up-regulated in NAFLD or in an HFD-induced fatty liver mice model (by more than 4-fold)<sup>6,7</sup>, but the mechanism was not evaluated. As a hepatic functional gene, up-regulation of *GSTM2* may function in hepatic

self-protection. Knockout and overexpression of *GSTM2* in a mouse model revealed its regulatory function in the development of hepatic steatosis. *GSTM2* KO enhanced the development of hepatic steatosis. Although *GSTM2* overexpression did not block the development of hepatic steatosis, it delayed the progression and reduced lipid accumulation and fibrosis progression. These results suggest that a liver with steatosis protects itself against disease injury by up-regulating *GSTM2*.

In addition to drug-induced toxicity, ROS is another metabolic by-product that can induce potential cytotoxicity. Many studies have demonstrated a relationship between ROS and lipid accumulation, particularly in fatty liver disease and hepatoma carcinoma<sup>28–30</sup>. Superoxide dismutase 1 (SOD1)-knockout mice showed higher hepatic fat storage, and more LDs were observed in SOD1 KO hepatocytes<sup>17,31</sup>. We also found that ROSup treatment induced greater LD formation in HepG2 cells in this study. As an



important cellular antioxidant, glutathione is responsible for eliminating ROS. Therefore, *GSTM2* can promote ROS degradation by enhancing the activity of glutathione, as demonstrated by our results. We predicted that *GSTM2* could alleviate ROS-induced neutral lipid accumulation and increase the fat content in NAFLD. Interestingly, in a previous study glomerulonephritis was treated by injecting *GSTM2*-transduced mesenchymal stem cells. The researchers found that *GSTM2* expression significantly reduced oxidation and inflammation in the disease tissues and greatly ameliorated glomerulonephritis<sup>32</sup>. In our study, we observed a lower occurrence of fibrosis in *GSTM2*-overexpressing mice than in control mice. This phenotype is attributed to the function of *GSTM2* which ameliorates cellular stress and inflammation. We detected the antioxidant expression level in the *GSTM2* KO mice model and found that most antioxidants including *SOD1*, *CAT*, and *GPX1* were down-regulated. The higher level of ROS and inflammation may impair the function and expression of these antioxidants. Notably, *GSTM1* shows high similarity in sequence and structure (>90%) to *GSTM2*, and Bhat-tacharjee et al. reported that *GSTM2* can play a compensatory role in the absence of *GSTM1*<sup>33</sup>. Indeed, *GSTM1* has a similar function as *GSTM2*, but several single-nucleotide polymorphisms may lead to gene inactivation. Moreover, no inactivating mutation of *GSTM2* has been found in human or house mouse. We considered that *GSTM2* was likely to be more stable than *GSTM1* from a genetic perspective, and therefore, up-regulating *GSTM2* may be a better choice for inducing protective effects.

We demonstrated that *GSTM2* suppressed the progression of hepatic steatosis by inhibiting ASK1-p38/JNK signalling. This signalling has been reported to play an important role in the development of NAFLD and NASH. ASK1, also known as MAP3K5, activates the downstream p38-JNK1/2 signalling pathway, thereby promoting inhibition of lipid and glucose metabolism<sup>34–36</sup> and driving a strong inflammatory response<sup>37</sup>. ASK1 is currently considered as a target site for NASH therapy<sup>38,39</sup>, and ASK1 signalling is abnormally active in the liver of NAFLD and obese individuals. Inhibition of ASK1 activity significantly inhibits the development of NASH. For example, selonsertib (GS-4997) is a highly selective and potent ASK1 inhibitor with potential anti-inflammatory, anti-tumour, and anti-fibrotic activities<sup>40</sup>. Clinical trial results of the patient showed that GS-4997 has a good therapeutic effect on NASH. However, GS-4997 completely inhibits the activity and normal function of ASK1 with potential side effects<sup>41,42</sup>. In our study, hepatic *GSTM2* was found to suppress steatosis by inhibiting ASK1-p38/JNK signalling. Moreover, *GSTM2* inhibits hepatic steatosis by affecting the capability to detoxify and function as an antioxidant. Some previous studies supported our results. Han et al. found that *GSTM2* expression was much higher in ovarian teratoma mesenchymal stem cell-like cells than in normal cells and that p38 was highly inhibited in the teratomas<sup>43</sup>. Some early references also described the function of GSTs in regulating the activity of kinases such as ASK1 via protein-protein interactions<sup>14,44–46</sup>. Currently, the effect of ASK1-p38/JNK signalling on NAFLD and NASH has attracted the attention of researchers. It is important to note that there are currently some negative results of ASK1-related small molecule inhibitors (such as CFLAR-mimicking peptide) in clinical trials. Some studies have observed that these small molecule inhibitors may promote inflammation and amplify NASH liver injury<sup>47</sup>. Our findings may provide new insights into the role of ASK1 in NAFLD and contribute to the development of related molecular agents.

We also investigated the effect of *GSTM2* on LD growth. Inhibition of *GSTM2* resulted in a significant increase in the diameter of LDs formed by cells in a fatty acid-rich environment, and thus *GSTM2* appears to affect the LD growth process. According to previous studies, LD growth depends on lipid synthesis genes such as *DGAT2* and *GPAT4*, and the key to the

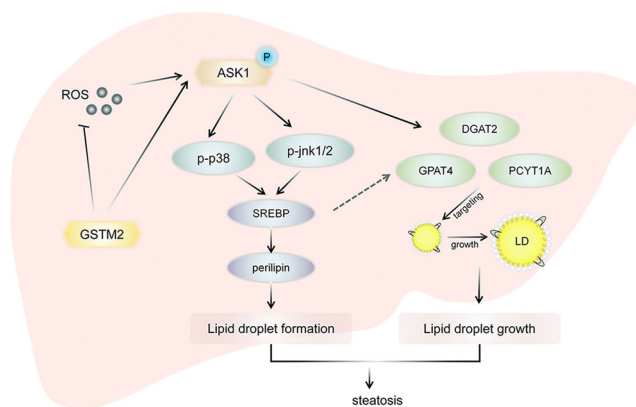


**Fig. 7** *GSTM2* protects against the development of hepatic steatosis via its antioxidant and suppressing ASK1-p38/JNK signaling. *GSTM2* was highly up-regulated in hepatic steatosis tissues. As the member of phase II drug metabolizing enzymes, *GSTM2* could detoxify the toxicity of metabolic products such as ROS. ROS could enhance the inflammation and fibrosis progression. Furthermore, *GSTM2* interacted with ASK1 directly and suppressed ASK1 phosphorylation. Therefore, *GSTM2* down-regulated expression of SREBP and perilipins to inhibit the LD accumulation. ASK1 signaling also regulated the expression level of *DGAT2*, *GPAT4* and *PCYT1A* and the recruitment of *DGAT2* and *GPAT4* on LD surface to modulate the LD growth. In conclusion, *GSTM2* protects against the hepatic steatosis of NAFLD via its antioxidant and suppressing ASK1-p38/JNK signaling.

growth of LDs is the recruitment of *DGAT2* and *GPAT4* to the LD surface<sup>18</sup>. We inhibited the expression of *GSTM2* and found that recruitment of *DGAT2* and *GPAT4* to the surface of LDs was increased. Because hydrogen peroxide treatment did not significantly affect the LD diameter, intracellular ROS may have minimal effects on LD growth. We further examined whether ASK1 signalling affects the LD growth process. When cells were treated with 400 mM palmitic acid or 5  $\mu$ M GS-4997, the recruitment of *DGAT2* and *GPAT4* on the surface of LDs showed significant differences. When ASK1 was activated, *DGAT2* and *GPAT4* were recruited to the LD surface, whereas when ASK1 activity was inhibited, recruitment of *GPAT4* to the surface of LDs was reduced. Therefore, ASK1 may affect the growth of LDs by affecting the recruitment of *DGAT2* and *GPAT4* to the LD surface. No previous studies reported the effect of *GSTM2* or ASK1-p38/JNK signalling on LD growth. This is the first study to demonstrate that ASK1-p38/JNK regulated LD growth by promoting *DGAT2* and *GPAT4* targeting to the surface of LDs. We did not investigate the mechanism of this regulatory role; therefore, further studies are needed.

In summary, we identified *GSTM2* as a protective factor against hepatic steatosis. *GSTM2* interacted with ASK1 and suppressed its phosphorylation and the activation of downstream p38-JNK signalling. Moreover, *GSTM2* plays an important role in detoxification and antioxidant activities, which protect tissues against injury induced by drugs or oxidative stress (Fig. 7). *GSTM2* showed a therapeutic effect on hepatic steatosis, providing a potential strategy for the clinical treatment of NAFLD.

## Materials and methods

**Animals and cell lines.** *GSTM2* knockout mice were prepared by Cyagen Bioscience, Inc. (Santa Clara, CA, USA). The C57/BL-6 mice were used for the knockout construction. One single-base deletion was induced in exon3 of the *GSTM2* (NM\_008183.3) gene using the TALEN method. All mice were housed in a normal environment and provided with food and water. The 6–8 week ages male mice were used in this study. All experimental protocols were approved by the

Ethics Committee of Huazhong Agricultural University. The HepG2 cell line was gifted by Xianghua Yan's lab (Huazhong Agricultural University).

**Ethics approval and consent to participate.** All mouse were housed in a normal environment provided with food and water. The methods were performed in accordance with the approved guidelines from Huazhong Agricultural University, and scientific, ethical and legal principles of the Hubei Regulations for the Administration of Affairs Concerning Experimental Animals. All experimental protocols were approved by the Ethics Committee of Huazhong Agricultural University.

**Antibodies.** The following rabbit polyclonal antibodies were used: anti-GSTM2 (#ab125,102, Abcam, Cambridge, UK, 1:1000), anti-GSTM2 (#A13,496, ABclonal, Wuhan, China, 1:2000), anti-GAPDH (#CSB-PA00025A0Rb Flarebio Biotech LLC, College Park, MD, USA, 1:1000), anti-CIDEA (#D222114, Sangon Biotech, Shanghai, China, 1:1000), anti-CIDEA (#12287-1-AP, Proteintech, Rocky Hill, NJ, USA, 1:1000), anti-ADRP/perilipin2 (#15294-1-AP, Proteintech), anti-DGAT2 (#bs-12,998R, BIOSS, Beijing, China), anti-DGAT2 (#A13,891, ABclonal, Wuhan, China, 1:2000), anti-GPAT4 (#bs-15,587R, BIOSS), anti-SREBP1 (#14,088-1-AP, Proteintech), and anti-PCYT1A (#bs-11306R, BIOSS), anti-PCYT1A (#A5935, ABclonal, Wuhan, China, 1:1000). The mouse monoclonal antibody used was anti-tubulin (#GB13017-2, Servicebio, Wuhan, China, 1:1000). The following secondary antibodies were used: Alexa Fluor 555-labelled donkey anti-rabbit IgG (H+L) (#A0453, Beyotime, Shanghai, China, 1:200), horseradish peroxidase (HRP)-labelled goat anti-rabbit IgG (H+L) (#GB23303-1, Servicebio, 1:8000), HRP-labelled goat anti-mouse IgG (H+L) (#GB23301, Servicebio, 1:8000), and HRP-conjugated goat anti-rabbit IgG (#D110,058, Sangon Biotech, 1:8000).

**Plasmid DNA construction.** Full-length coding sequences encoding *GSTM2* (NM\_001142368.1) and *PCYT1A* (NM\_005017.3) were amplified using a cDNA library of HepG2 cells and then subcloned into the pcDNA3.1 vector (gifted from Prof. Dequan Xu's lab, Huazhong Agricultural University) and pEGFP-C1 and pmCherry-C1 vectors (gifted from Prof. Xianghua Yan's lab, Huazhong Agricultural University). Sequences of the primers used for the *GSTM2* RNAi experiment were referred to study of Huenchuguala<sup>48</sup>. The sequences were subcloned into the pSuperior.puro vector for the RNAi experiment (gifted from Prof. Xianghua Yan's lab).

**Cell culture and transfection.** WT HepG2 or stably transfected cells (pSuperior.puro-GSTM2) were cultured in DMEM (HyClone, Logan, UT, USA) containing 10% foetal bovine serum (Clark Bioscience, Richmond, VA, USA), 100 U/mL penicillin, and 100 g/mL streptomycin in dishes at 37 °C and transfected with Lipofectamine 2000 Transfection Reagent (#C0528, Beyotime). HepG2 cells were seeded onto a cell slide in a 24-well plate and transfected with plasmid vectors according to the transfection reagent instructions.

**HE staining and Oil Red O staining of histological sections.** For HE staining, the liver tissues of three *GSTM2* knockout mice and three wild-type mice were divided and fixed in 4% paraformaldehyde for 12 h. Then the samples were performed the HE and Oil Red O staining by Servicebio (Wuhan, China) (<http://www.servicebio.com/>).

**ROS level detection.** Cells were seeded into a 96-well black plate. ROS levels in the cells were detected using an ROS Assay Kit (#S0033, Beyotime) based on the DCFH-DA method. The ROS level was detected using a microplate spectrophotometer (PerkinElmer EnSpire, Waltham, MA, USA). The excitation and emission wavelengths were 488 and 525 nm, respectively. ROSup was used as an activator to increase the ROS level in cells, which was added to the wells at 1:1000 (v:v) with DMEM and incubated at 37 °C.

**Western blot and real-time PCR.** Real-time PCR was performed using a Roche LightCycler 480 detection system (Roche, Basel, Switzerland). One negative control reaction in which the cDNA template was replaced with water was performed as a control. Each sample was amplified in triplicate, and the comparative Ct ( $\Delta\Delta Ct$ ) value method was used for relative quantification. GAPDH was used as a reference gene. The Western blot method referred to our previous study<sup>49</sup>.

**Immunofluorescence assay.** The immunofluorescence method referred to our previous study<sup>49</sup>. The confocal laser scanning microscope (Carle Zeiss, German) was used to observe the slide of cells. The images were analysed by ZEN pro software (Carle Zeiss, German), ImageJ and Photoshop CS6 (Adobe).

**Living cells workstation.** The cells were seeded into a 35 mm confocal dish for 24 h culture and OA treatment, and then were washed 3 times with PBS and then added to the DMEM culture containing BODIPY (1:1000, v/v), followed by incubation for 20 min at 37 °C. The dish was placed in a living cell workstation, and intracellular LDs were observed using a 63 × oil immersion objective. The exposure

time was set to 200 ms, the definitely focused 2.0 strategy was used, the interval of image capture was 15 s, and the duration of capture was 1 h. The data were analysed using ZEN pro and ZEN 2.3 (blue edition) software (ZEISS, Oberkochen, Germany).

**HFD and MCDD feeding experiment.** Fifteen 4-week-old healthy male *GSTM2* knockout mice and 15 wild-type mice were selected for high-fat diet (HFD) feeding. The mice were divided into five groups of 3 individuals each. The mice were sacrificed on days 0, 5, 10, 20, and 30 after the start of HFD feeding and then liver tissues were collected. The formula of the HFD was ordinary mixed diet (88.5%), lard (10%), cholesterol (1%), and pig bile salt (0.5%). Six-week-old male mice were divided into two groups and fed an MCDD. The tissue collection was conducted as described above.

**Triglyceride content detection.** The TG content of the liver tissues was detected by fully automatic chemistry analyser (#Chemray 240, Rayto Life and Analytical Sciences Co.,Ltd., Shenzhen, China). The total protein concentration was detected by Enzyme Label Detector (#Epoch, BioTek Instruments, Inc., headquartered in Winooski, VT, USA). The TG content data was normalized by protein concentrations, mmol/g.

**Plasmid and inhibitor injection.** The *GSTM2* overexpression or control plasmid (200 µg) was mixed with HiGene I (14.4 µL) (#C1507, Applygen Technologies Inc., Beijing, China). Then the mixture was incubated at room temperature (RT) for 30 min. The mixture was injected intraperitoneally. By detection of *GSTM2* expression in liver, skeletal muscle, heart and brain, no significant change was observed except in liver tissues. In addition, 5 mg of GS-4997 (also called selonsertib; #S8292, Selleck, Shanghai, China), an ASK1 inhibitor, was mixed with 1 mL of dimethyl sulfoxide (DMSO) to prepare the 10 mM mother liquor. Then the mother liquor was diluted by normal saline for 80 µM working fluid, and the inhibitor was injected intraperitoneally.

**Statistics and reproducibility.** All experiments were repeated three times. Data are shown as the mean ± SD. Student's *t*-test was used for statistical comparisons. For experiments comparing more than two groups, one-way ANOVA and two-way ANOVA were used. *P* value < 0.05 was considered as statistically significant.

**Reporting summary.** Further information on research design is available in the Nature Research Reporting Summary linked to this article.

## Data availability

The source data for all the graphs in main figures in Supplementary Data 1. The data used to support the findings of this study are available from the corresponding author upon request.

Received: 9 May 2021; Accepted: 11 March 2022;

Published online: 06 April 2022

## References

- Thompson, M. D. et al. Enhanced steatosis and fibrosis in liver of adult offspring exposed to maternal high-fat diet. *Gene Expr.* **17**, 47–59 (2016).
- Sherif, Z. A. et al. Global epidemiology of nonalcoholic fatty liver disease and perspectives on US minority populations. *Dig. Dis. Sci.* **61**, 1214–1225 (2016).
- Loomba, R. & Sanyal, A. J. The global NAFLD epidemic. *Nat. Rev. Gastro Hepat.* **10**, 686–690 (2013).
- Beuckmann, C. T., Fujimori, K., Urade, Y. & Hayaishi, O. Identification of Mu-class glutathione transferases M2-2 and M3-3 as cytosolic prostaglandin E synthases in the human brain. *Neurochem. Res.* **25**, 733–738 (2000).
- Chanas, S. A. et al. Loss of the Nrf2 transcription factor causes a marked reduction in constitutive and inducible expression of the glutathione S-transferase *Gsta1*, *Gsta2*, *Gstm1*, *Gstm2*, *Gstm3* and *Gstm4* genes in the livers of male and female mice. *Biochem. J.* **365**, 405–416 (2002).
- Si, X., Strappe, P., Blanchard, C. & Zhou, Z. Enhanced anti-obesity effects of complex of resistant starch and chitosan in high fat diet fed rats. *Carbohydr. Polym.* **157**, 834–841 (2017).
- Wang, C., Tao, Q., Wang, X., Wang, X. & Zhang, X. Impact of high-fat diet on liver genes expression profiles in mice model of nonalcoholic fatty liver disease. *Environ. Toxicol. Pharmacol.* **45**, 52–62 (2016).
- Saify, K., Saadat, I. & Saadat, M. Down-regulation of antioxidant genes in human SH-SY5Y cells after treatment with morphine. *Life Sci.* **144**, 26–29 (2016).

9. Huenchuguala, S. et al. Glutathione transferase mu 2 protects glioblastoma cells against aminochrome toxicity by preventing autophagy and lysosome dysfunction. *Autophagy*. **10**, 618–630 (2014).
10. Cuevas, C. et al. Glutathione transferase-M2-2 secreted from glioblastoma cell protects SH-SY5Y cells from aminochrome neurotoxicity. *Neurotox. Res* **27**, 217–228 (2015).
11. Huenchuguala, S., Muñoz, P. & Seguraaguilar, J. The importance of mitophagy in maintaining mitochondrial function in U373MG cells. bafilomycin a1 restores aminochrome-induced mitochondrial damage. *ACS Chem. Neurosci.* **8**, 2247–2253 (2017).
12. Li, D. J. et al. Melatonin safeguards against fatty liver by antagonizing TRAFs-mediated ASK1 deubiquitination and stabilization in a beta-arrestin-1 dependent manner. *J. pineal Res.* **67**, e12611 (2019).
13. Dorion, S., Lambert, H. & Landry, J. Activation of the p38 signaling pathway by heat shock involves the dissociation of glutathione S-transferase Mu from Ask1. *J. Biol. Chem.* **277**, 30792 (2002).
14. Cho, S. G. et al. Glutathione S-transferase Mu modulates the stress-activated signals by suppressing apoptosis signal-regulating kinase 1. *J. Biol. Chem.* **276**, 12749–12755 (2001).
15. Dolado, I. et al. p38 alpha MAP kinase as a sensor of reactive oxygen species in tumorigenesis. *Cancer Cell*. **11**, 191–205 (2007).
16. Liu, L. et al. Glial lipid droplets and ROS induced by mitochondrial defects promote neurodegeneration. *Cell*. **160**, 177–190 (2015).
17. Kurahashi, T. et al. An SOD1 deficiency enhances lipid droplet accumulation in the fasted mouse liver by aborting lipophagy. *Biochem. Biophys. Res. Commun.* **467**, 866–871 (2015).
18. Wilfling, F. et al. Arf1/COPI1 machinery acts directly on lipid droplets and enables their connection to the ER for protein targeting. *ELife*. **3**, e01607 (2013).
19. Guo, Y. et al. Functional genomic screen reveals genes involved in lipid-droplet formation and utilization. *Nature*. **453**, 657–661 (2008).
20. Krahmer, N. et al. Phosphatidylcholine Synthesis for lipid droplet expansion is mediated by localized activation of CTP:phosphocholine cytidyltransferase. *Cell Metab.* **14**, 504–515 (2011).
21. Xiong, X. W., Tao, R. Y., DePinho, R. A. & Dong, X. C. The autophagy-related gene 14 (Atg14) is regulated by forkhead box o transcription factors and circadian rhythms and plays a critical role in hepatic autophagy and lipid metabolism. *J. Biol. Chem.* **287**, 39107–39114 (2012).
22. Yang, L., Li, P., Fu, S. N., Calay, E. S. & Hotamisligil, G. S. Defective hepatic autophagy in obesity promotes  $\beta$  stress and causes insulin resistance. *Cell Metab.* **11**, 467–478 (2010).
23. Li, P. et al. Hepatic pharmacokinetics of cationic drugs in a high-fat emulsion-induced rat model of nonalcoholic steatohepatitis. *Drug Metab. Dispos.* **39**, 571–579 (2011).
24. Tarantino, G., Di Minno, M. N. D. & Capone, D. Drug-induced liver injury: is it somehow foreseeable? *World J. Gastro.* **15**, 2817–2833 (2009).
25. Fisher, C. D. et al. Experimental non-alcoholic fatty liver disease results in decreased hepatic uptake transporter expression and function in rats. *Eur. J. Pharm.* **613**, 119–127 (2009).
26. Zhang, W. V., Ramzan, I. & Murray, M. Impaired microsomal oxidation of the atypical antipsychotic agent clozapine in hepatic steatosis. *J. Pharm. Exp. Ther.* **322**, 770–777 (2007).
27. Tarantino, G. et al. A prospective study of acute drug-induced liver injury in patients suffering from non-alcoholic fatty liver disease. *Hepatol. Res.* **37**, 410–415 (2007).
28. Videla, L. A., Rodrigo, R., Araya, J. & Poniachik, J. Insulin resistance and oxidative stress interdependency in non-alcoholic fatty liver disease. *Trends Mol. Med.* **12**, 555–558 (2006).
29. Gawrieh, S., Opara, E. C. & Koch, T. R. Oxidative stress in nonalcoholic fatty liver disease: Pathogenesis and antioxidant therapies. *J. Invest. Med.* **52**, 506–514 (2004).
30. Videla, L. A. et al. Oxidative stress-related parameters in the liver of non-alcoholic fatty liver disease patients. *Clin. Sci.* **106**, 261–268 (2004).
31. Lee, J., Homma, T., Kurahashi, T., Kang, E. S. & Fujii, J. Oxidative stress triggers lipid droplet accumulation in primary cultured hepatocytes by activating fatty acid synthesis. *Biochem. Biophys. Res. Commun.* **464**, 229–235 (2015).
32. Li, Y. J. et al. Glutathione S-transferase Mu 2-transduced mesenchymal stem cells ameliorated anti-glomerular basement membrane antibody-induced glomerulonephritis by inhibiting oxidation and inflammation. *Stem Cell Res. Ther.* **5**, 19 (2014).
33. Bhattacharjee, P. et al. Functional compensation of glutathione S-transferase M1 (GSTM1) null by another GST superfamily member, GSTM2. *Sci. Rep.* **3**, 2704 (2013).
34. Sun, P. et al. Caspase recruitment domain protein 6 protects against hepatic steatosis and insulin resistance by suppressing Ask1. *Hepatology*. **68**, 2212–2229 (2018).
35. Ye, P. et al. Dual-specificity Phosphatase 9 Protects Against Non-alcoholic Fatty Liver Disease in Mice via ASK1 Suppression. *Hepatology*. **69**, 76–93 (2018).
36. Lawan, A. et al. Hepatic mitogen-activated protein kinase phosphatase 1 selectively regulate glucose metabolism and energy homeostasis. *Mol. Cell. Biol.* **35**, 26 (2015).
37. Cingolani, F. & Czaja, M. J. Oxidized albumin—a Trojan Horse for p38 MAPK-mediated Inflammation in decompensated Cirrhosis. *Hepatology*. **68**, 1678–1680 (2018).
38. Nakagawa, H. et al. Apoptosis signal-regulating kinase 1 inhibits hepatocarcinogenesis by controlling the tumor-suppressing function of stress-activated mitogen-activated protein kinase. *Hepatology*. **54**, 185–195 (2011).
39. Win, S. et al. New insights into the role and mechanism of c-Jun-N-terminal kinase signaling in the pathobiology of liver diseases. *Hepatology*. **67**, 2013–2024 (2017).
40. Loomba, R. et al. The ASK1 inhibitor selonsertib in patients with nonalcoholic steatohepatitis: a randomized, phase 2 trial. *Hepatology*. **67**, 549–559 (2018).
41. Villanueva, M. T. Liver disease: conscious uncoupling in NASH. *Nat. Rev. Drug Discov.* **16**, 238 (2017).
42. Nishida, T., Hattori, K. & Watanabe, K. The regulatory and signaling mechanisms of the ASK family. *Adv Biol. Regul.* **66**, 2–22 (2017).
43. Han, I. et al. Proteomic analysis of mesenchymal stem-like cells derived from ovarian teratoma: potential role of glutathione S-transferase M2 in ovarian teratoma. *Proteomics*. **11**, 352–360 (2011).
44. McIlwain, C. C., Townsend, D. M. & Tew, K. D. Glutathione S-transferase polymorphisms: cancer incidence and therapy. *Oncogene*. **25**, 1639–1648 (2006).
45. Ichijo, H. et al. Induction of apoptosis by ASK1, a mammalian MAPKKK that activates SAPK/JNK and p38 signaling pathways. *Science*. **275**, 90–94 (1997).
46. Hsieh, C. C. & Papaconstantinou, J. Thioredoxin-ASK1 complex levels regulate ROS-mediated p38 MAPK pathway activity in livers of aged and long-lived Snell dwarf mice. *Faseb J.* **20**, 259–268 (2006).
47. Loomba, R., Friedman, S. L. & Shulman, G. I. Mechanisms and disease consequences of nonalcoholic fatty liver disease. *Cell*. **184**, 2537–2564 (2021).
48. Huenchuguala, S. et al. Glutathione transferase mu 2 protects glioblastoma cells against aminochrome toxicity by preventing autophagy and lysosome dysfunction. *Autophagy*. **10**, 618–630 (2014).
49. Jin, Y., Tan, Y. J., Chen, L. P., Liu, Y. & Ren, Z. Q. Reactive oxygen species induces lipid droplet accumulation in HepG2 cells by increasing perilipin 2 expression. *Int. J. Mol. Sci.* **19**, 3445 (2018).

## Acknowledgements

This work was supported by the National Key Research and Development Program of China (2021YFF1000601), the National Natural Science Foundation of China (32172700) and the Joint Funds of the National Natural Science Foundation of China (U20A2052), and the Fundamental Research Funds for the Central Universities (grant number 2662018PY043).

## Author contributions

Y.J. and Z.-Q.R. participated in research design; Y.J., Y.-J.T., P.-X.Z., Y.G. and S.-L.C. performed experiments; Y.J. drafted the paper; Y.-J.T., J.W. and Z.-Q.R. contributed to the writing of the manuscript and supervised the study. All authors read and approved the final manuscript.

## Competing interests

The authors declare no competing interests.

## Additional information

**Supplementary information** The online version contains supplementary material available at <https://doi.org/10.1038/s42003-022-03251-w>.

**Correspondence** and requests for materials should be addressed to Jian Wu or Zhuqing Ren.

**Peer review information** *Communications Biology* thanks the anonymous reviewers for their contribution to the peer review of this work. Primary Handling Editors: Gabriela da Silva Xavier and Karli Montague-Cardoso.

**Reprints and permission information** is available at <http://www.nature.com/reprints>

**Publisher's note** Springer Nature remains neutral with regard to jurisdictional claims in published maps and institutional affiliations.



**Open Access** This article is licensed under a Creative Commons Attribution 4.0 International License, which permits use, sharing, adaptation, distribution and reproduction in any medium or format, as long as you give appropriate credit to the original author(s) and the source, provide a link to the Creative Commons license, and indicate if changes were made. The images or other third party material in this article are included in the article's Creative Commons license, unless indicated otherwise in a credit line to the material. If material is not included in the article's Creative Commons license and your intended use is not permitted by statutory regulation or exceeds the permitted use, you will need to obtain permission directly from the copyright holder. To view a copy of this license, visit <http://creativecommons.org/licenses/by/4.0/>.

© The Author(s) 2022